ILC-Asia-2006-01
May, 2006
Linac, Cavity, Tuning

# Estimation of Lorentz Detuning and Related Tuning Characteristics of ICHIRO Cavity

T. Higo, Y. Higashi, Y. Morozumi, H. Yamaoka and K. Saito (KEK)

# Estimation of Lorentz detuning and related tuning characteristics on ICHIRO cavity

T. Higo, Y. Higashi, Y. Morozumi, H. Yamaoka and K. Saito

**Abstract**

Lorentz detuning was calculated for a low-loss cavity for ILC, the ICHIRO cavity. The detuning amounts to 3kHz when operated at 45MV/m. The compensation can be done by a tuner integrated in a helium vessel. The static and dynamic compensation characteristics were estimated. In the case that the tuner moves linearly, the loss in transient frequency response shift is only 30% with respect to the static response at the end of the ramping time of 1 msec.

# 1. Intorduction

The acceleration in the main linac of ILC[1], International Linear Collider, is based on the super-conducting cavity at 1.3GHz. Some analysis on the optimum field from the cost point of view indicates a cost minimum at around 40MV/m[2]. The higher accelerating field becomes, the shorter the length of the linac becomes, and the shorter linac is preferable from total site size point of view[3].

One of the most important issues for the cavity operation at such a high field is the compensation of the cavity resonant frequency shift within a pulse. The cavity wall suffers from a large Maxwell's stress which is proportional to the square of the field. This results in the cavity deformation resulting in a frequency change called Lorentz detuning. Since the pulse width for ILC is as long as 1.6msec, the cavity can be mechanically deformed within the period. Therefore in a pulse operation, the transient frequency shift is inevitable. It was realized that the amount of this Lorentz detuning varies from cavity to cavity by a factor of 2 in TTF and this situation has not been analyzed well enough to understand the scattering[4]. This paper tried to estimate the relevant parameters taking the ICHIRO cavity, a low-loss cavity for ILC.

There are various analyses based on mechanical resonance mode of the cavity system[5]. In this paper, we analyzed the cavity system directly using 3D mechanical analysis code, ANSYS[6], for the deformation associated various processes. The deformation obtained is used to estimate the frequency shift using Slater's perturbation theory[7]. This analysis was done for each cell out of 9 cells in a cavity.

In addition, the analysis of external mechanical force to compensate this Lorentz detuning was performed. Both static and transient analyses were performed.

## 2. Calculation formula

*Estimation of frequency change due to surface deformation*

Frequency change can be estimated by using Slater's perturbation theory in the case that the global field pattern does not change much. This condition is fulfilled usually in the superconducting cavity operation. Following formula were taken in this note.

Maxwell's stress $$S = -\frac{1}{2}\varepsilon_0(E_z^2 + E_r^2) + \frac{1}{2}\mu_0 H_\varphi^2$$

Slater's perturbation theory $$\delta F / F = \frac{1}{2}\int_{all\ volume} \frac{S}{U} dV = \frac{1}{2}\int_{cell\ contour} \frac{S}{U} \cdot 2\pi r\, ds\, dn,$$

where $$U = Stored\ Energy = \frac{1}{2}\varepsilon_0(E_z^2 + E_r^2) + \frac{1}{2}\mu_0 H_\varphi^2,$$

and $$R/Q = \frac{(Eacc \cdot Lacc)^2}{\omega U}.$$

## 3. Mechanical configuration of ICHIRO cavity

*ICHIRO cavity shape*

The ICHIRO cavity shape is shown in Fig. 1[8]. The left side is called “inner side” and the right side “outer side” in this note. We name the cells from the left end cell to the right end cell as from #1 to #9. Cell dimensions are summarized in http://lcdev.kke.jp.

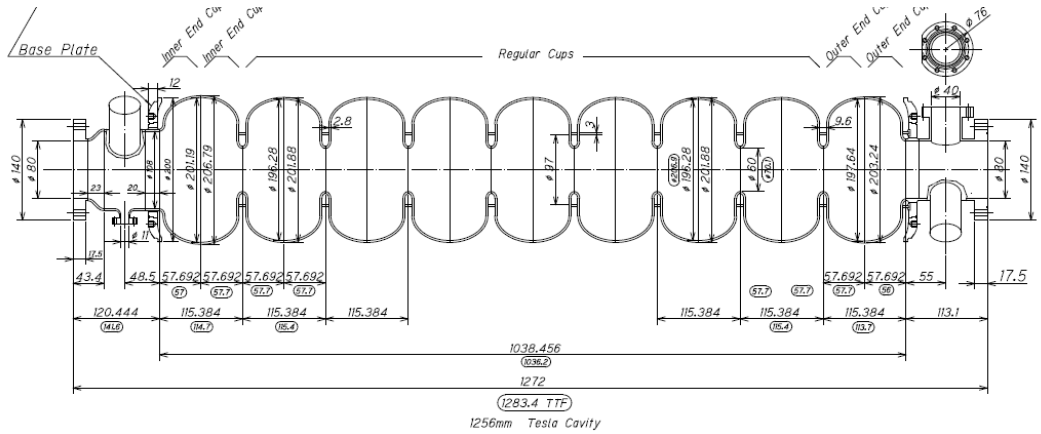


**Fig. 1 Bare ICHIRO cavity.**

Each gap between cells is equipped with a stiffening ring. The same ring is attached between cell #9 and the end plate while no stiffening is applied between the left end cell and the end plate. The calculated z-direction stiffening of this system is calculated to be 1840N/mm.

The cavity in use is covered by a Helium jacket with some tuner mechanism integrated. The stiffness of the system of a tuner, jacket and end plate system is calculated to be N/mm.

Table 1. Z-direction stiffness of Ichiro cavity related parts. (Units are kN/mm.)

| Item | Stiffness | Comments |
|---|---|---|
| Bare Ichiro cavity | 1.84 | With stiffener |
| Tuner/jacket/end plates | 59.7 | |
| (Left end plate) | (114) | |
| (Right end plate) | (195) | |
| (Jacket) | (295) | 2mm thick |
| (Coaxial tuner) | (5000) | Higashi priv. Comm. |
| Total system | 1.785 | |

## 4. Frequency response to axial expansion of a cavity

The amount of the Lorentz detuning and the related cavity tuning processes are largely connected to the frequency response to the expansion/shrinkage of the 9-cell cavity. Here we estimate the sensitivity.

The deformation of a cavity when pushed by the end flange is calculated by ANSYS. The Fig. 2 shows typical cell deformation patterns by picking up the center cell. Blue dots in the left figure are deformed position with 200 times expanded. This deformation plot was shifted to make the z-coordinate of the cell center unchanged indicated by green points to estimate the effect to the frequency change of each cell. The actual frequency shift is the sum of the convolution of the deformed volume toward the direction normal to the surface (left figure) and the Maxwell's stress there.

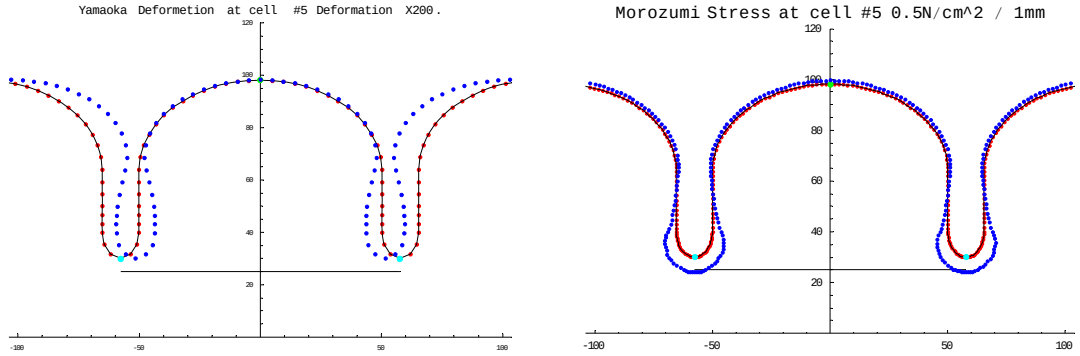


**Fig. 2 Left: Deformation of center cell. Right: Maxwell's stress of center cell.**

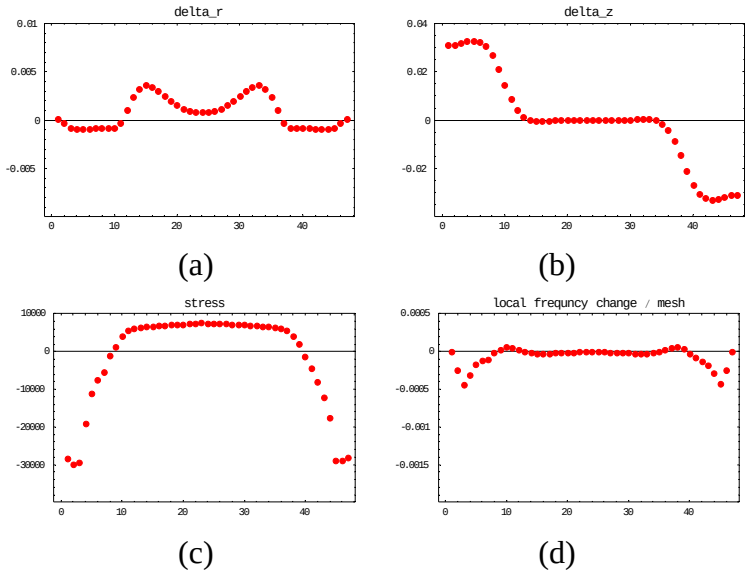


**Fig. 3 Frequency shift of the center cell. (a) Radial deformation. (b) Axial deformation. (c) Maxwell's stress. (d) Frequency shift associated to each mesh.**

The frequency shift of each cell can be analyzed as that of the center cell shown above. Main contribution to the frequency shift is that from the iris area, while the radial deformation of the equator and the surrounded area does not contribute much. In Fig. 4 is plotted the frequency shift of each cell. The contribution of the cell #1 is small comparing to the other cells because the large beam pipe prevents one of the iris deformation. The summation of these values makes the frequency sensitivity of the cavity as a whole to be 368kHz/mm.

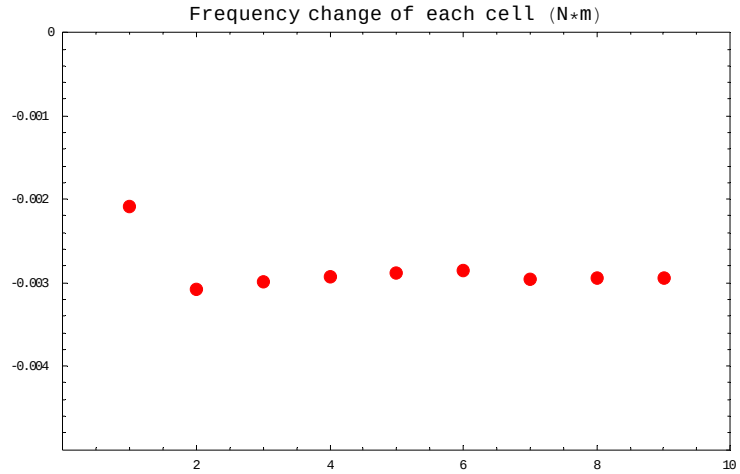


**Fig. 4 Frequency shift attributed to each cell frequency shift due to shrinkage of 9-cell cavity.**

## 5. Lorentz detuning of regular cell

*Single cell analysis (periodic boundary condition)*

The Maxwell's stress distribution in a cell is shown in Fig. 6. An estimation of Lorentz detuning was performed on a regular cell. Both ends were fixed in z-direction. The result is shown in Fig. 5. The area around iris is push inward due to large electric field, while the equator area is pushed outward due to magnetic field. The stiffening ring is attached at the radial position 50mm from the z-axis so that the deformation at the stiffening ring is very small.

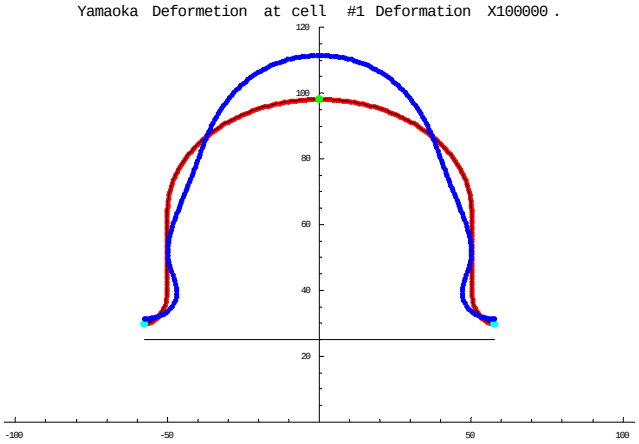


**Fig. 5 Deformation due to Maxwell's stress.**
**Red line shows cavity design contour, while blue shows the deformed shape.**

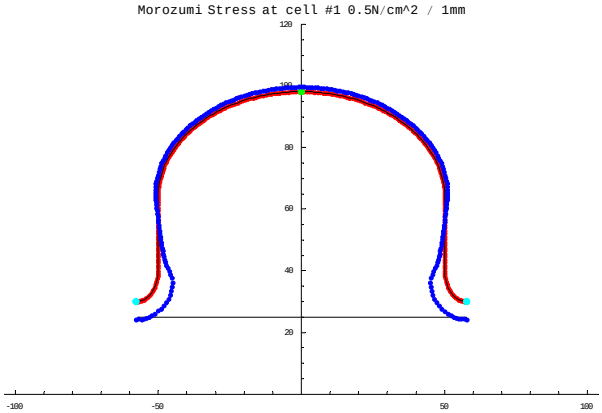


**Fig. 6 Maxwell's stress distribution is shown by blue point. The amount for each point is shown by the deviation of the blue point from the red one along the normal direction from the red point. Inward direction shows frequency lowering, while outer frequency increase.**

The frequency change for each mesh line is calculated as shown in Fig. 7. This is the convolution of Figs. 2 and 3. The resultant frequency shift is obtained from the summation of all the mesh lines. The obtained value is

$$\Delta F_{LD} = - 1.726 \text{ kHz at } 45 \text{MV/m}$$

or

$$k_{LD} = - 0.852 \text{ kHz / (MV/m)}^2.$$

It is worthwhile to remind that this value is for the case that the both ends are fixed in z-direction.

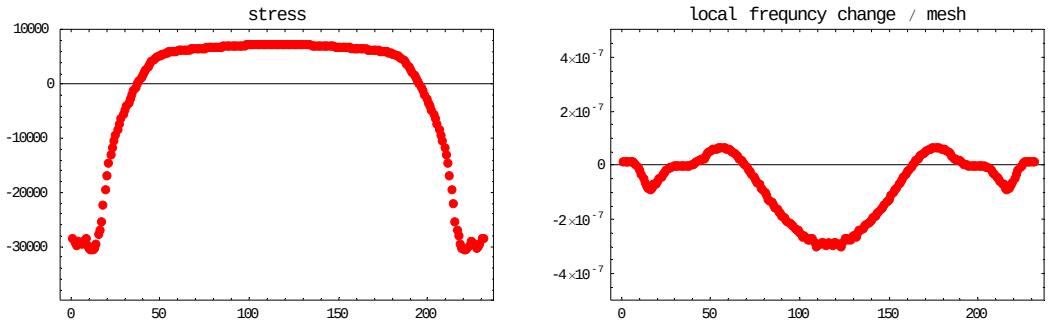


**Fig. 7 Left figure shows Maxwell's stress distribution along surface points. Right figure shows the product of Maxwell's stress and associated deviation in the normal direction. Horizontal axis is the mesh number along surface.**

The amount of the Lorentz detuning of an actual 9-cell cavity should be close to this value.

# 6. Steady-state Lorentz detuning of 9-cell cavity

## *6.1 ICHIRO cavity field*

The surface field of ICHIRO cavity at Eacc=45MV/m is shown in Fig. 8. The typical Maxwell's stress distribution is shown in Fig. 2.

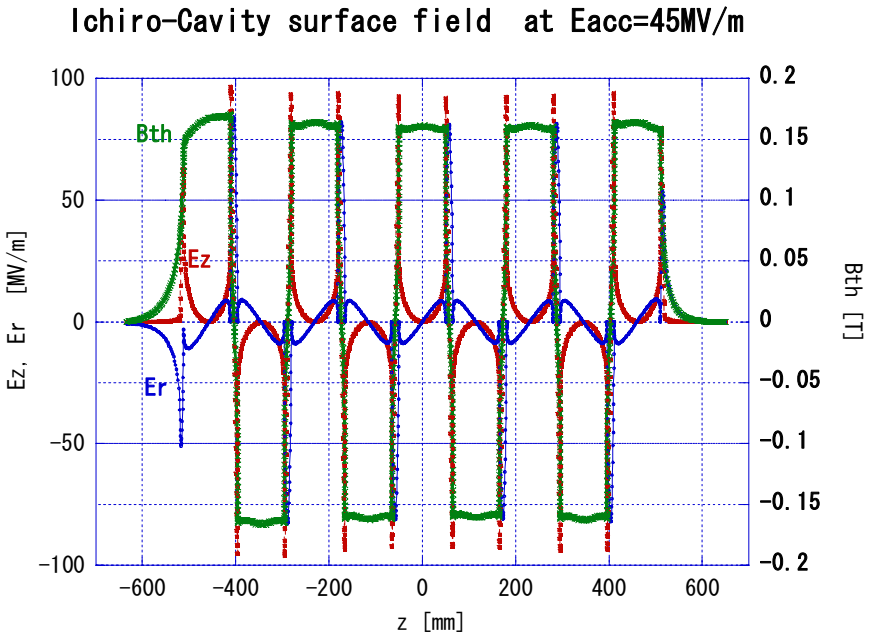


**Fig. 8 Surface field of ICHIRO cavity.**

## *6.2 Process of estimating Lorentz frequency shift*

Firstly we made a calculation of deformation due to Maxwell's stress with both ends of a cavity free. In this condition, the total shrinkage becomes $\Delta L_{shrink}$ = 56 microns and the frequency shift amounts to $\Delta F_{LD}$ = -23.8 kHz at Eacc = 45 MV/m. If we take the static tuning sensitivity of 368Hz/micron, then the detuning with both ends fixed in z-direction becomes - 3.2kHz. However, this way of estimation subjects to big error because of the subtraction of big numbers to get a small value. Because the stiffness of the system of tuner and He vessel is much larger than that of the cavity, this large error is inevitable. Therefore, we took another way of estimation.

In order to get the value in a more precise manner, we made another deformation

simulation with both end fixed as the starting point. The associated frequency shift due to this deformation is then calculated as described in section 2. Secondly, the axial force received by the cavity due to Maxwell's stress is calculated from the total shrinkage of the cavity by using the stiffness of the cavity. Then the shrinkage of the actual cavity equipped with a tuner and He vessel is calculated. The associated frequency shift due to this cavity shrinkage is calculated taking the static sensitivity of section 4 into account.

### *6.3 Static Lorentz detuning estimation with both ends fixed*

The ANSYS simulation was performed on the 9-cell cavity with two end points fixed in z-direction. The stress is given by the Maxwell's stress at 38.4MV/m. The result on the deformation is shown in the following figures. The deformation of each cell is shown independently by shifting the actual shape in z-direction so that the middle of each cell coincides with the point without deformation.

By integrating from the middle of the left iris to the middle of the right iris, the frequency shift due to the deformation of the cell is evaluated. The integration for the end cell is extended into beam pipe.

#### *Center cell*

The deformation and resultant frequency shift for the center cell are shown in the following figures. In Fig. 9 are shown the Maxwell's stress distribution and the deformation due to the stress. In Fig. 10 are shown the stress of each mesh along the contour and the associated frequency shift attributed to each mesh.

As seen in these figures, the electromagnetic field makes the frequency of the cell lower by the iris part shrunk in the axial direction and the cell equator with its neighboring area expanded outerward in radial direction. On the other hand, some area between iris and equator makes the frequency higher due to the deformation sprung back toward inner side due to the existence of the stiffening ring. The overall frequency shift of the cells is negative.

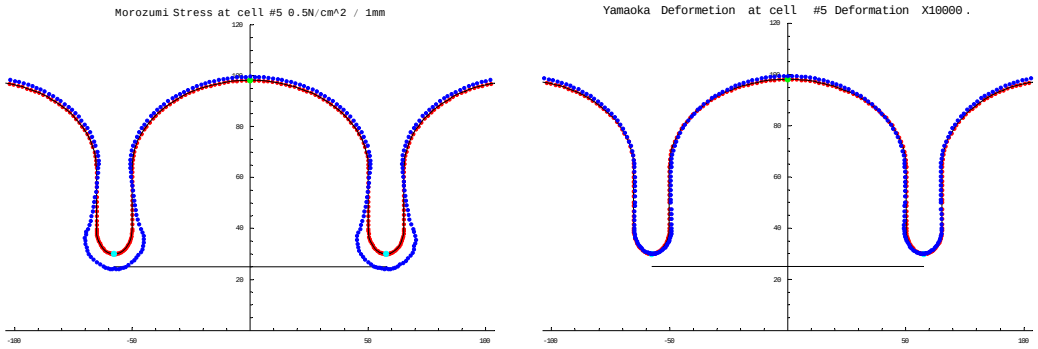


**Fig. 9 Left: Maxwell's stress distribution at center cell and Right: resultant deformation magnified by 10000 times.**

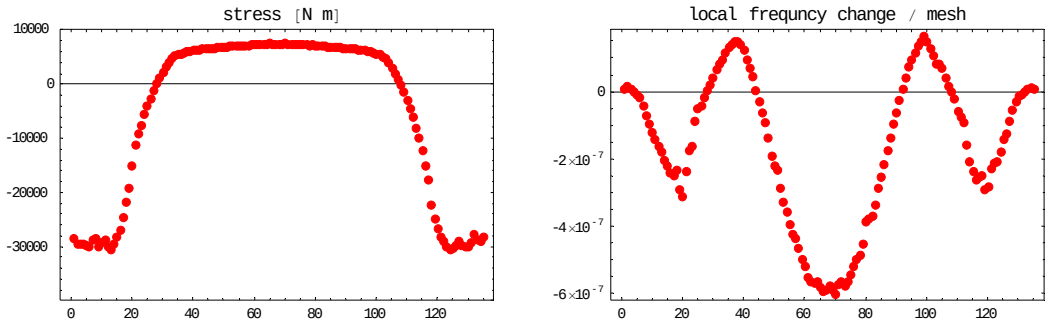


**Fig. 10 Left: Frequency sensitivity for each mesh point. Right: Resultant frequency shift of each mesh.**

*Left end cell #1*

The distribution of the deformation and Maxwell's stress of the left end cell is shown in Fig. 11. The resultant frequency shift is shown in Fig. 12. The total frequency shift of the cell is negative.

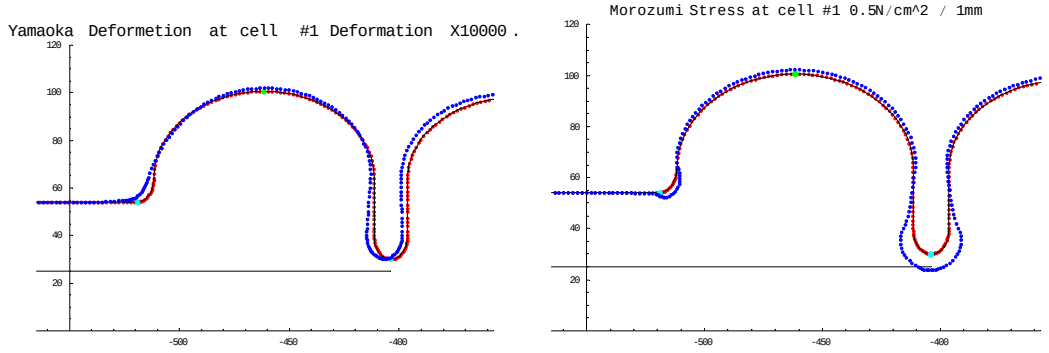


**Fig. 11 Left: Deformation due to static Lorentz detuning of the left end cell. Right: Maxwell's stress distribution of the cell.**

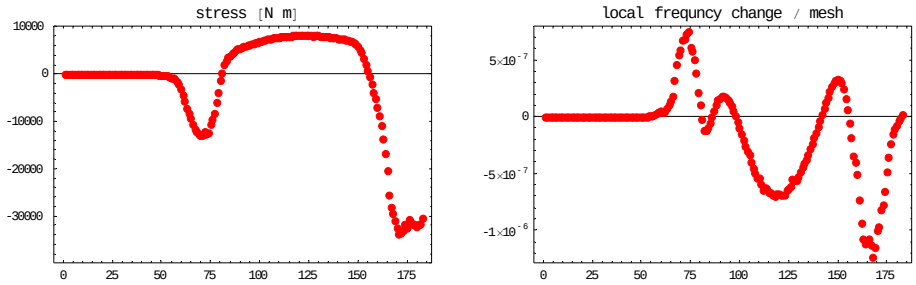


**Fig. 12 Left: Frequency sensitivity of each mesh point. Right: Resultant frequency shift.**

*Right end cell*

The distribution of the deformation and Maxwell's stress of the left end cell is shown in Fig. 13. The resultant frequency shift is shown in Fig. 14. The total frequency shift of the cell is negative.

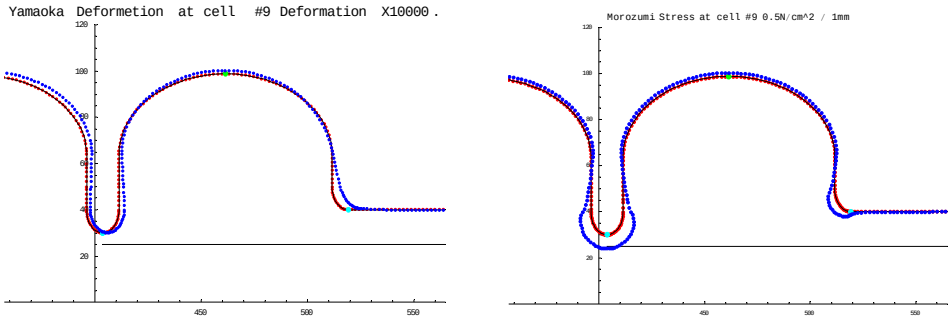


**Fig. 13 Left: Deformation due to static Lorentz detuning of the cell. Right: Maxwell's stress distribution at right end cell.**

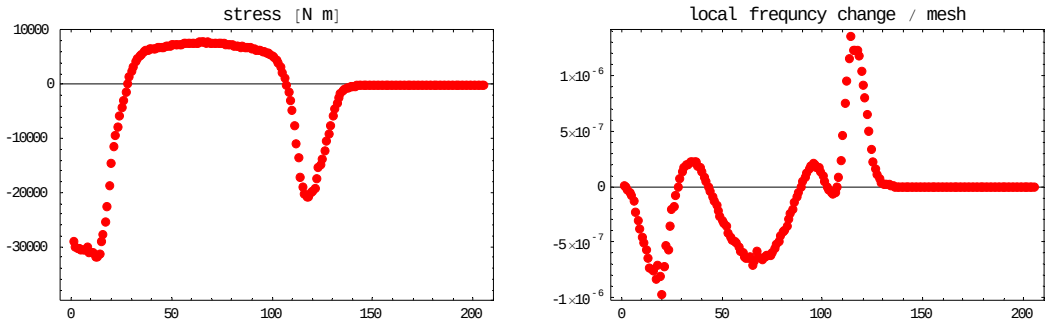


**Fig. 14 Left figure shows frequency sensitivity for each mesh point. Right figure shows the product of Maxwell's stress and the deformation due the stress for each mesh point.**

*Detuning as a whole cavity with both ends fixed*

Fig. 15 shows the distribution of frequency change of each cell. By adding these nine values, we obtain the detuning amount as a whole cavity with fixed end condition as

$k_{LD}$ = - 1.175 Hz / $(MV/m)^2$

or

$\Delta F_{LD}$ = - 2.38 kHz at 45MV/m.

This value is 74% of that obtained in section 6.2 and crudely agrees with the above result, which confirms the process of the frequency shift estimation. We consider that the above value is more precise than that of section 6.2 and we take the above one as the representative value. This is

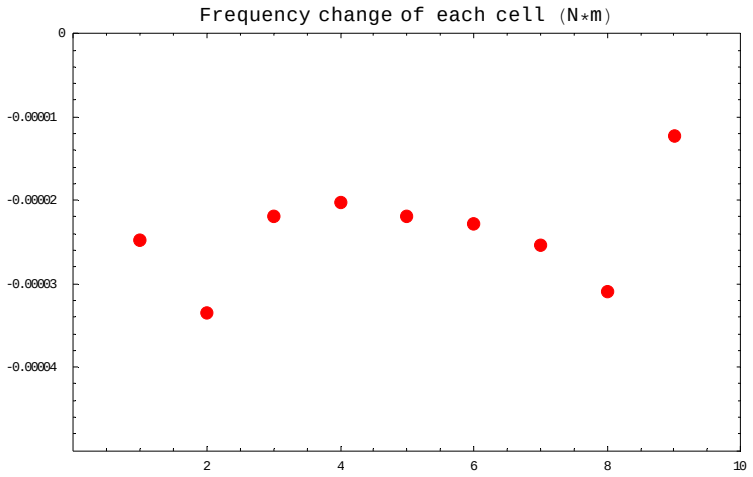


**Fig. 15 Distribution of frequency shift among all cells. (at Eacc=38.4MV/m)**

### *6.4 Estimation of actual Lorentz detuning of a cavity equipped with tuner/jacket*

The axial pressure due to the Maxwell's stress is calculated as

Axial pressure = 56 microns * 1.84 kN/mm = 103 N,

where the total shrinkage of a cavity is obtained in section 6.2 while the stiffness of a cavity is listed in Table 1. The resultant shrinkage of the actual cavity is calculated using the stiffness of the cavity system listed in the same table.

Shrinkage of an actual cavity = 103 N / 59.7 (kN/mm) = 1.73 micron.

Then, the frequency shift due to this shrinkage is calculated by using the static frequency sensitivity obtained in the section 4 as

Frequency shift due to shrinkage = 1.73 micron * 368 kHz/mm = 637Hz.

Finally, the frequency shift of the actual cavity can be obtained as the sum of the frequency shift with two ends fixed (section 6.3) and the effect due to the shrinkage of the cavity system described above as

$\Delta F_{LD}$ = - 2.379kHz - 637Hz = - 3.016kHz  at 45MV/m,

or

$k_{LD}$ = - 1.489 kHz / (MV/m)^2.

Summarizing all the frequency shift calculations, the results are listed in table2. Some relevant mechanical values are also listed in Table 3.

Table 2.  Frequency shift due to Maxwell's stress in various cases.

| Frequency shift | $\Delta F_{LD}$ | $k_{LD}$ |
|---|---|---|
| | at 45 MV/m | Sensitivity |
| Units | kHz | Hz / (MV/m)^2 |
| Single cell with both ends fixed | - 1.73 | - 0.85 |
| Cavity with two ends fixed | - 2.38 | - 1.18 |
| Actual cavity with tuner and jacket | - 3.02 | - 1.49 |

Table 3.  Relevant values related to Lorentz detuning at 45MV/m.

| Item | Values | Units |
|---|---|---|
| Shrinkage of a bare cavity | 56 | microns |
| Total axial force due to Maxwell's stress | 103 | N |
| Shrinkage of actual cavity with tuner and jacket | 1.73 | micron |

## 7. Transient Lorentz detuning of 9-cell cavity

The transient Lorentz detuning is estimated by assuming the both ends of the cavity fixed in z-direction. This assumption can be applied in case the stiffness of the tuner+jacket system is large enough. The accelerating field is ramped with Qex=2.6 $10^6$, followed by a constant field after 0.571msec. The transient deformation of the cavity is calculated by ANSYS. The frequency shift at each time is evaluated in the same manner as in Chapter 2. The frequency shifts of each cell at eight timings are shown in Fig. 16. The timings correspond to those marked in the next Fig. 17.

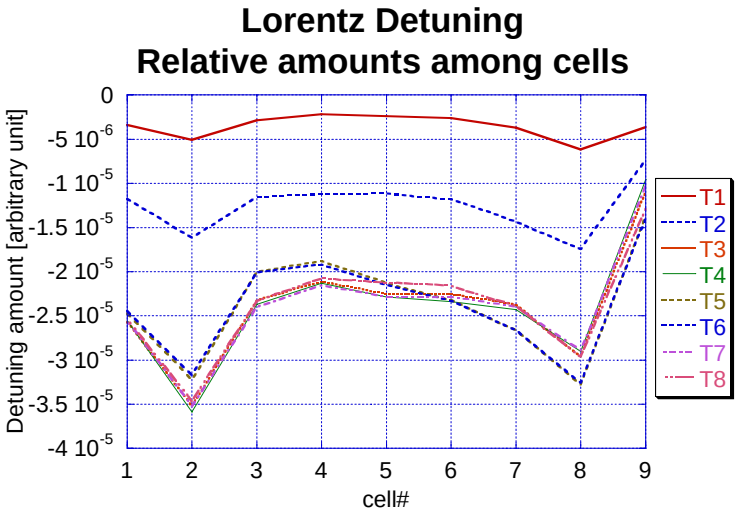


**Fig. 16 Frequency shift of each cell at various timing of time-varying field.**

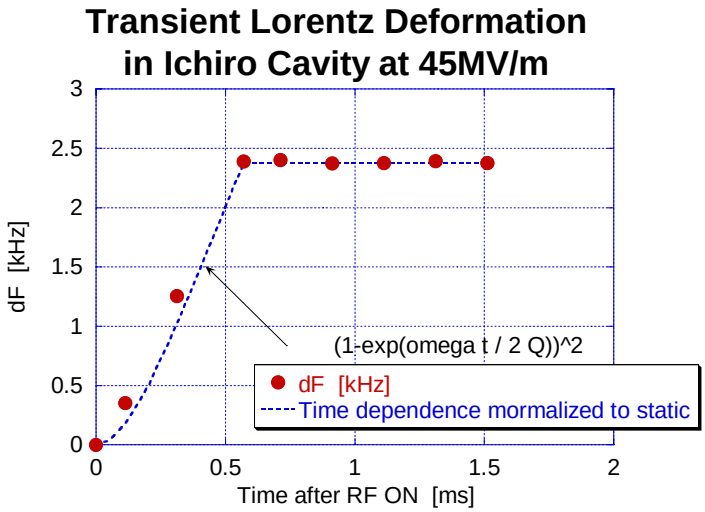


**Fig. 17 Frequency shift of the cavity (red dots) and the field squared (blue dashed line).**

Various information were obtained from these result.

1. The steady state Lorentz detuning value in Chapter 6 agrees well to the transient analysis value after 0.57msec.
2. The second cell and the eighth cell give large contribution, while the end cells, especially the right end cell, are small.
3. The Lorentz detuning follows almost proportional to the accelerating field squared.

# 8. Frequency compensation methods

## *8.1 Static frequency compensation*

The frequency of a cavity can be increased by axially pulling the cavity. The sensitivity was calculated in Chapter 4. The uniformity of this tuning is very good except for the left end cell, whose sensitivity is 70% of the other cell. This deviation of cell frequency is only ~100Hz in case of 3kHz tuning as a whole, which is negligibly small comparing to the bandwidth of the accelerating mode passband. Therefore, the field uniformity is kept preserved.

## *8.2 Transient compensation*

### *Response to bare cavity by pushing end flange*

Firstly, a bare cavity (without tuner nor jacket) is analyzed on transient linear tuner response. Here the left end flange is fixed and the right end flange is moved linearly in time by 1 micron during 1 msec.

The associated deformation is shown in Fig. 18, where only right end and the next cell are perturbed. The time evolution of the deformation is found in Fig. 19. In 0.5msec duration, the deformation appears in the last cell fully and the next a little. At 1 msec later, the deformation appears in the 7$^{th}$ cell and the right two cells are deformed fully. The resultant frequency change is also shown in the same figure and the above description of the propagation of the deformation appears in the cell frequency shift, also shown in the same figure with red dots.

The summary of this transient frequency shift is listed in the column of “without jacket” in Table 4.

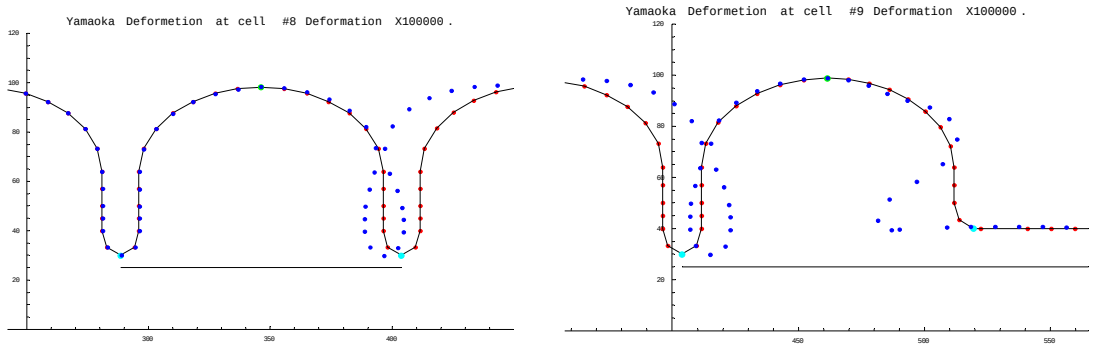


**Fig. 18 Cavity deformation by pushing right end flange with left end fixed in z-direction. Left: cell #8, next from the right end cell. Right: Right end cell.**

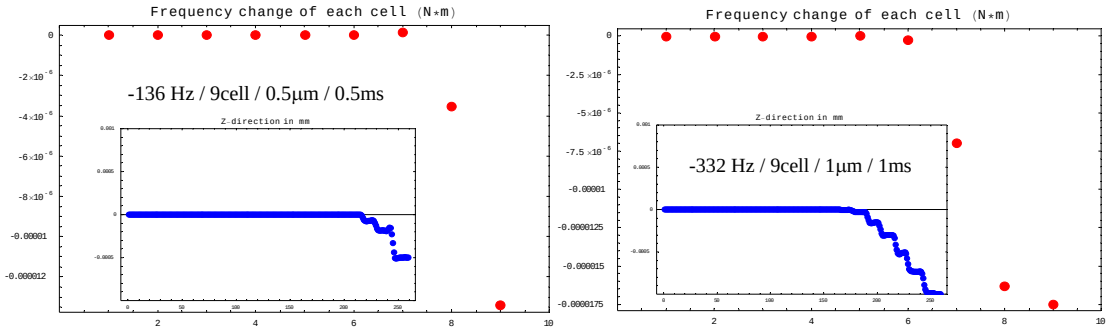


**Fig. 19 Deformation in z-direction at time 0.5 and 1 msec by pushing right end. Red dots are associated cell frequency change.**

## *Response to tuner with jacket*

Transient tuner response in a realistic configuration shown in Fig. 20 is then calculated. The tuner is assumed to be expanded as shown in the figure with linear ramping in time within 1 msec. The deformations at the time 0.5 msec and 1 msec are analyzed to estimate the amount of the frequency tuning. The typical deformation pattern of the left side of the cavity at 0.5msec later is shown in Fig. 21. It is seen that only the left side cell is deformed. At the right end, the situation is the same that only the right end cell is deformed. Very little movement occurs in the middle cells.

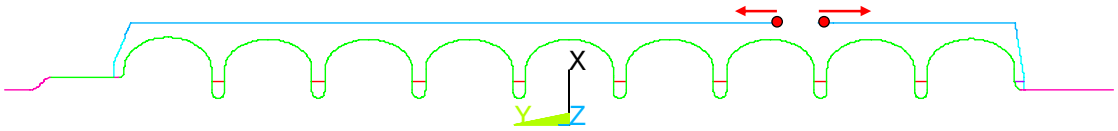


**Fig. 20 Configuration of the cavity system, tuner, end plates and He jacket, for tuner transient calculation with ANSYS.**

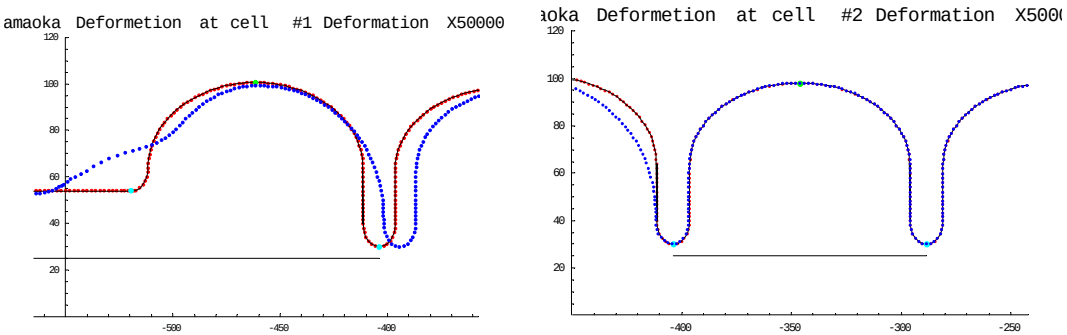


**Fig. 21 Deformation of left end cell and the next cell at the last moment of the linear ramping at the time 0.5msec.**

This situation is clearly shown in Fig. 22, where the deviation in z-direction is shown along whole cavity. When 1 msec passes, we estimate that the next cell from the end cell will begin deformed a little, which is speculated from Fig. 19. The corresponding frequency shift for each cell at 0.5 msec is shown in Fig. 23. As anticipated, only both two end cells contribute to the frequency shift. The obtained tuner responses on frequency shift at 0.5 msec and 1 msec are summarized in Table 4.

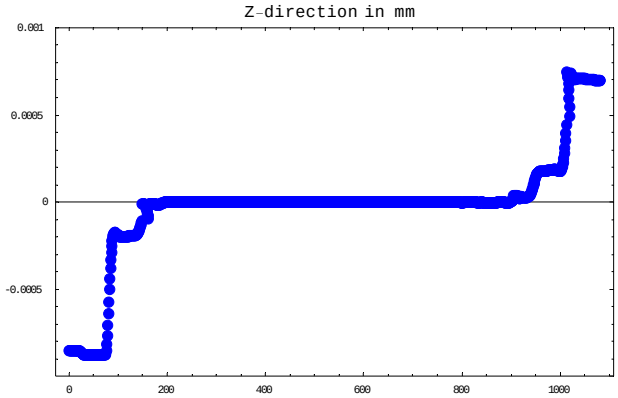


**Fig. 22 Deformation of a cavity in z-direction at the time 0.5msec after tuner linear ramping.**

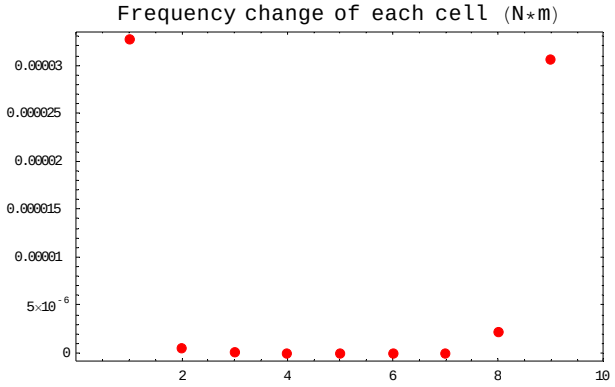


**Fig. 23 Cell frequency shift due to transient tuning after linear ramping for 0.5 msec.**

Table 4 Frequency change due to linear movement of tuner.

| Timing | 0.5ms | 1.0ms | Static |
|---|---|---|---|
| Total deformation | 0.5micron | 1.0micron | 1.0micron |
| Without jacket (bare cavity) | 136 Hz | 332 Hz | 368 Hz |
| Freq. perturbed cell | #9 | #8, #9 | All cells |
| With jacket | 125 Hz | 280 Hz | |
| Freq. perturbed cell | #1, #9 | #1, #2,#8,#9 | |

To summarize visually, the external compensation mechanism and associated frequency is shown in Fig. 24. As shown in the figure, it was found that the ratio of the frequency shift with respect to the static value increased from 68% to 76% during ramping time from 0.5ms to 1ms for the case of realistic configuration of cavity with tuner and jacket. Therefore, the tuner should be designed with an overhead of about 30% depending on how quickly the cavity should be tuner according to the ramping pattern of the accelerating field. It is to be noted that this rather fast frequency tuning is realized because the main contribution to this tuning comes from the deformation only at the end cells and NOT from the deformation at the middle of the cavity, where more time is needed for the mechanical deformation wave to propagate to reach.

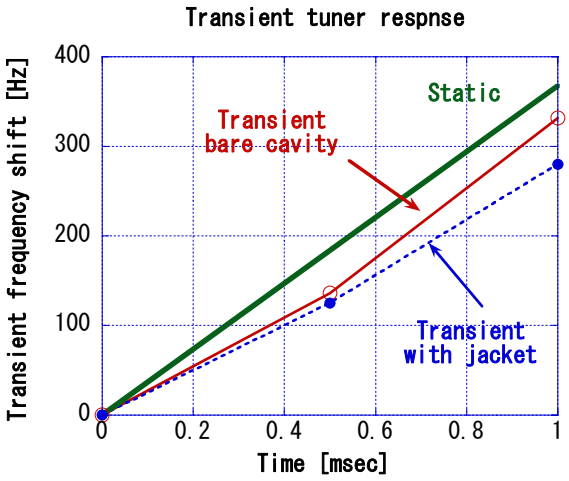


**Fig. 24 Transient frequency response to linear movement of tuner moving at 1μm/msec.**

## 7. Summary

The Lorentz detuning of a low-loss cavity system, ICHIRO cavity, was estimated. The Lorentz detuning amounts to 3kHz when operated at very high field such as 45MV/m.

The compensation of this frequency detuning is performed by pulling cavity with tuner equipped in a Helium jacket. For the static estimation, the amount is almost proportional to the product of total length of the cavity and the static frequency sensitivity. In the transient tuning case with ramping time of the order of 1 msec, the loss in frequency shift with respect to the static value is 24% at 1 msec or 32% at 0.5 msec. In this time range, only the end cells and the next cells are deformed by tuner transient movement.

## References


[1] ILC Web site, http://www.linearcollider.org/cms/.
[2] T. Raubenheimer's talk, MAC, FNAL, 2006, http://ilcagenda.cern.ch/conferenceDisplay.py?confId=290.
[3] K. Saito and M. Yoshioka, "Proposal for TeV-Superconducting Linear Collider", Proc. 1st Annual Meeting of Particle Accelerator Society of Japan and the 29th Linear Accelerator Meeting in Japan, Funabashi, Japan, 2004, http://lam29.lebra.nihon-u.ac.jp/proceedings.html.
[4] Discussed at Snowmass meeting in 2008, http://www-conf.slac.stanford.edu/snowmass05/proceedings/proceedings.html, and described in BCD, http://www.linearcollider.org/wiki/doku.php?id=bcd:bcd_home.
[5] E. Chishiro et al., "Modelling of Resonant Frequency Vibration of Superconducting Cavity", Proc. 2nd Superconducting Linear Accelerator Meeting in Japan, KEK Proceedings 99-25, p41, 2000.
[6] ANSYS
[7] J. C. Slater, "Microwave Electronics", p80, D. Van Nostrand Co., Inc., 1950.
[8] Detailed information of ICHIRO cavity can be retrieved in Morozumi's talk in 7th WG5-Asia meeting on 17 Dec. 2004, http://lcdev.kek.jp/ILC-AsiaWG/WG5notes/.